MECHANICAL PROPERTIES OF $MoSi_2$-Al_2O_3 COMPOSITES PROCESSED BY SHS

A.L. Dumont, J.P. Bonnet, and C. Gault

Groupe d'Etude des Matériaux Hétérogènes, ENSCI
47 Avenue Albert Thomas, 87065 Limoges, France

SUMMARY : $MoSi_2$-Al_2O_3 composites have been processed using a SHS technique assisted by the application of a low uniaxial pressure to achieve densification. $MoSi_2$ - rich composites (21 vol.% Al_2O_3), intermediate composition (56.1 vol.% Al_2O_3) and Al_2O_3 - rich composites (68.1 vol.% Al_2O_3) have been fabricated. In this paper, their mechanical properties (elastic moduli and creep behaviour) are investigated and discussed considering microstructure. Young's and shear moduli have been measured using an ultrasonic pulse-echo method. Their zero porosity values, extrapolated from experimental results are found to be inferior to the theoretical values predicted by a two-phase model. This is attributed to the influence of intergranular phases and/or microcracks. Compressive creep measurements have been performed in air in the 50-200 MPa and 1150-1400 °C ranges. Pseudo-stationary stages are observed with two different regimes characterised by different stress exponent values depending on the stress level.

KEYWORDS : elasticity, ultrasonics, creep, molybdenum disilicide, alumina, Self Heating Synthesis.

INTRODUCTION

Among intermetallics, $MoSi_2$ has received a great deal of attention for structural applications at high temperature because of its high oxidation resistance and of its high strength with a melting temperature exceeding 2000°C [1]. Additionally, $MoSi_2$ materials are electric conductors which gives them electro-discharge machinability and possibilities of use as resistors of electrical furnaces. The two main drawbacks for both structural and electrical applications are the dramatic sensitivity to oxidation at intermediate temperature (~500°C), the so-called pest oxidation [2], and a poor creep resistance above 1000°C [3]. Consequently solutions have been researched by processing $MoSi_2$-based composites exhibiting a good electrical conductivity without pest phenomenon and with an improved creep resistance. Among them, most of works have been concerned with reinforcement by SiC particles or whiskers [4]. The $MoSi_2$-Al_2O_3 system is also attractive because the two materials have similar thermal expansion and elastic properties, are chemically compatible, and because of the high creep resistance of Al_2O_3. Moreover an improvement of toughness by a classical particle-crack interaction can be expected. This paper deals with mechanical properties, elastic moduli at room temperature and creep compressive behaviour up to 1400°C, of $MoSi_2$-Al_2O_3 composites of various compositions processed by Self-propagating High-temperature Synthesis (SHS). The results are discussed and interpreted considering the microstructure and its evolution at high temperature.

EXPERIMENTAL

Fabrication and characteristics of the composites

Three compositions, C_1, C_2, C_3, with increasing Al_2O_3 content (see Table 1) have been synthesised. The reactive powders (containing MoO_3, Al, Si or SiO_2, Al_2O_3 or/and $MoSi_2$) were mixed in alcohol, dried and pressed into cylindrical pellets (25 mm diameter, 15-16 mm height, 52-59% green densification). Samples were placed in a graphite die and the SHS reaction was ignited at room temperature in air by the mean of an electrical resistor embedded in 2g of a highly exothermic mixture placed on the upper face of the pellet. Once the high-temperature reaction wave (>2000°C) had reached the bottom of the pellet, the densification of the sample was assisted by applying a low uniaxial pressure (typically 7 MPa) for about 15 min, until the sample was cooled. Details of the process are given elsewhere [5,6]. According to the fabrication conditions (particularly the loading procedure), the apparent porosities of the obtained composites range between 4 and 19 %, and SEM observations have shown an increasing density of cracks for increasing Al_2O_3 content.

Table 1: compositions and characteristics of the tested $MoSi_2$-Al_2O_3 composites.

Reference	Al_2O_3 content		density range (kg/m^3)	porosity range (%)
	mol.%	vol.%		
C_1	20	21	4550-5300	6 - 19
C_2	54.5	56.1	3980-4600	4 - 17
C_3	66.7	68.1	3600-4100	7 - 19

Microstructural investigations have been performed by X-ray diffraction (XRD) and EDS analyses and SEM observations. The composites are constituted of an homogeneous distribution of inclusions (≤ 60 µm) of the minor phase inside the matrix. For composition C_1, the $MoSi_2$-based matrix is composed of $MoSi_2$ grains surrounded by an Mo_5Si_3 intergranular phase. Traces of $Mo(Si,Al)_2$ grains can also be detected by XRD. The inclusions are alumina grains with a small amount of amorphous silico-aluminate intergranular phase. For C_2 and C_3, the matrix is composed of α-alumina grains surrounded by a silico-aluminate phase. EDS indicated a Si/Al atomic ratio of about 12%. Mullite is sometimes weakly detected by XRD. The inclusions are made of $MoSi_2$ or $Mo(Si,Al)_2$ grains. A Mo_5Si_3 phase can also be observed in intergranular position. Very small (1-3 µm) silicon-rich inclusions are sometimes detected by XRD in the matrix. Typical microstructures observed by SEM are given in Figures 1 and 2.

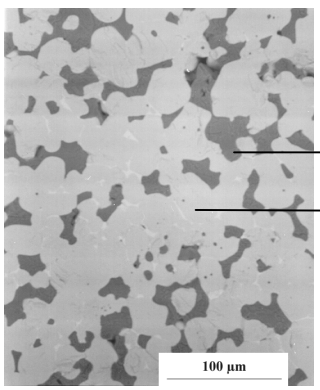

Fig. 1 : Backscattered electron micrograph of the typical microstructure of composite C_1

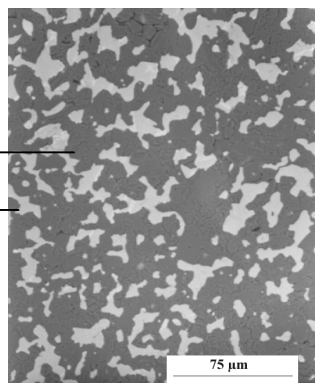

Fig. 2 : Backscattered electron micrograph of the typical microstructure of composite C_3

Ultrasonic measurements of elastic moduli at room temperature

Young's and shear moduli of samples of the three compositions have been evaluated from the measurement of velocities of longitudinal and shear ultrasonic waves (V_L and V_T resp.), using a classical pulse-echo technique working in a 10-15 MHz frequency range. Samples were 3-4 mm thick disks (15 mm diameter) with two parallel polished faces. Measurements of times of flight t_L and t_T between two successive echoes were made with a pulse-echo overlap method [7]. Knowing the sample thickness l, V_L and V_T are given by :

$$V_{L,T} = 2l / t_{L,T} \quad (1)$$

Then, Young' modulus E and shear modulus G are obtained from the following equations (ρ is the density of the material) :

$$E = \rho.[3V_L^2-4V_T^2] / [(V_L^2/V_T^2)-1] \quad (2)$$

$$G = \rho.V_T^2 \quad (3)$$

The experimental error on t is ñ5 ns, precisions on thickness and density measurements are 0.3% and 1%, therefore precisions are 8% for E and 3% for G.

Compression creep tests

Creep experiments were carried out in air under a constant uniaxial compression load, using a lever-arm testing machine working up to 1450°C [5]. Samples were parallelepipedic bars of $3\times3\times7$ mm^3 loaded on their greatest length. The strain was evaluated from the relative displacement of the two loading fixtures using a linear variable differential transformer (LVDT) with a sensitivity of $\pm$ 0.5 μm.
Two kinds of tests have been performed in air : the ones at constant temperature (1150°C and 1200°C) under increasing loads in the range 50-200 MPa, the others under a constant stress of 50 MPa with 6 temperature jumps in the range 1100-1400°C.

RESULTS AND DISCUSSION

Elastic properties of the composites

The results of measurements of the elastic moduli are plotted as a function of porosity on Figures 3, 4 and 5 for composites C_1, C_2 and C_3 respectively.
For each composition elastic moduli are found to decrease approximately linearly within the experimental errors, when porosity increases. Values for completely dense materials, Eo(exp) and Go(exp), have been extrapolated at zero porosity. The errors on Eo(exp) and Go(exp) are obtained from the two extreme slopes of experimental variation (dotted lines). Poisson's ratio ν_0(exp) has been calculated from Eo(exp) and G_0(exp) using the wellknown equation :

$$\nu_0(exp) = [E_0(exp)/2G_0(exp)]-1 \quad (4)$$

Unfortunately, ν_0(exp) is obtained with a very high experimental error and it can only be concluded that it is of the same order of magnitude than the ones of pure $MoSi_2$ (ν=0.17) and pure Al_2O_3 (ν=0.22).
These results are summed up in table 2.

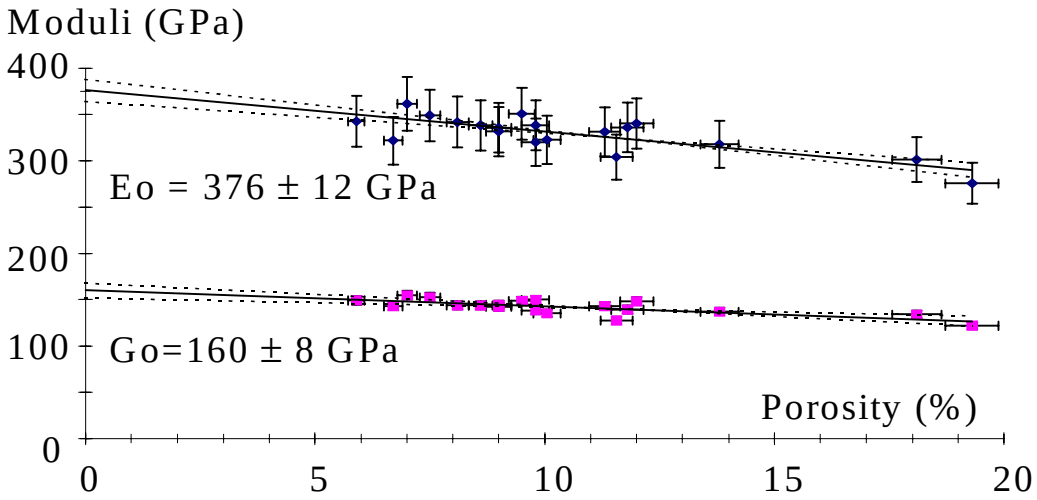

Fig.3: Elastic moduli versus porosity for C_1

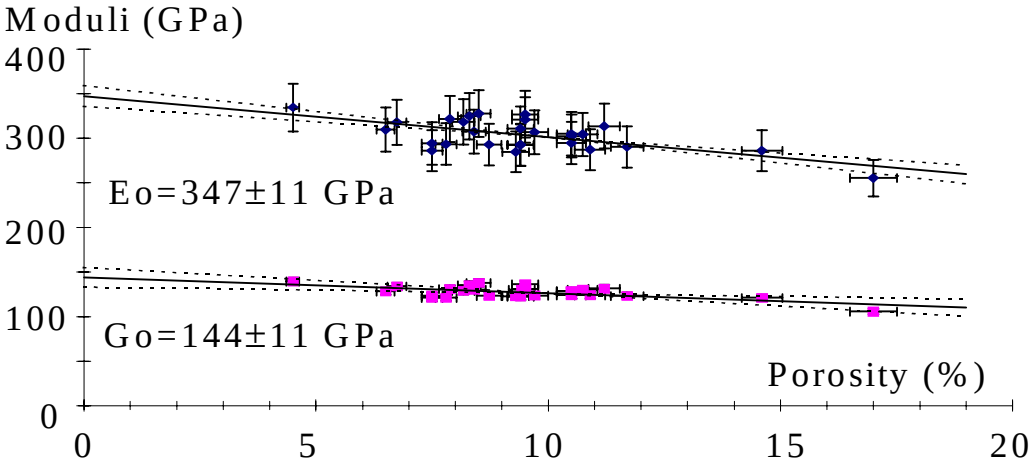

Fig. 4 : Elastic moduli versus porosity for C_2

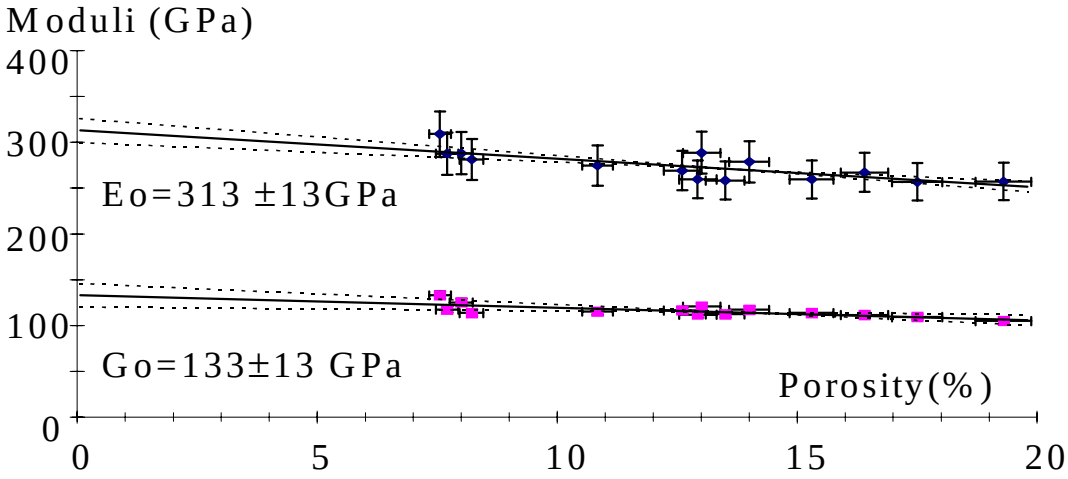

Fig. 5 : Elastic moduli versus porosity for C_3

For an hypothetical two-phase dense material with perfect bonding between the phases, Voigt and Reuss equations give upper and lower bounds M_V and M_R for the prediction of elastic moduli. The calculation for Young's modulus assumes that both phases have the same Poisson's ratios. Then, for $MoSi_2$-Al_2O_3 composites :

$$M_V = v_a \cdot M_a + (1- v_a) \cdot M_m \quad (5)$$
$$M_R = M_a \cdot M_m / [v_a \cdot M_m + (1- v_a) \cdot M_a] \quad (6)$$

M being Young's or shear modulus, v being fractional volume and suffixes a and m being related to Al_2O_3 and $MoSi_2$ respectively.

Values of v_a for each composition are given in Table 1. The elastic moduli of pure, dense, polycrystalline Al_2O_3 and $MoSi_2$ are respectively E_a=403 GPa, G_a=163 GPa, E_m=440 GPa and G_m=191 GPa. They have been taken from literature results theoretically evaluated from the elastic constants of single crystals [7-10]. As mentioned above, the elastic properties of $MoSi_2$ and Al_2O_3 are very close. Assuming that Poisson's ratio of both constituents are identical, the calculation of the theoretical values E_V, E_R, G_V, G_R has been made using equations (5) and (6). In all cases, Voigt and Reuss bounds are very close (± 1 GPa). Therefore, the rounded to unit arithmetic means, Eo(th) and Go(th), have been considered to be representative of ideal dense $MoSi_2$-Al_2O_3 composites. Their values are given in Table 2 for comparison with experimental values.

Table 2 : comparison of experimental results and theoretical values of zero porosity elastic parameters of the composites

Composition	Eo(exp) (GPa)	Go(exp) (GPa)	ν_0 (exp)	Eo(th) (GPa)	Go(th) (GPa)
C_1	376 ± 12	160 ± 8	0.18 ± 0.08	432	185
C_2	347 ± 11	144 ± 11	0.20 ± 0.1	419	175
C_3	313 ± 13	133 ± 13	0.18 ± 0.13	415	171

As expected, when the alumina content increases, the theoretical values of the moduli decrease, but Eo(exp) and Go(exp) are always lower than Eo(th) and Go(th). Moreover, the gap increases as the alumina content increases. Two causes could be responsible for this effect :

- an increase of the crack array of the composite when the alumina content increases ;
- the presence of the intergranular phase with low elastic constants, which could increase as the alumina content increases.

The first cause could be a result of the thermal shock during the process. Indeed, after the SHS reaction, as the combustion wave has converted the reactants into products, the composite naturally cools in its crucible. The temperature decreases from 2000°C to room temperature in about 20 minutes. As $MoSi_2$ is ductile down to about 1000°C, at high temperature its resistance to thermal shocks is higher than that of alumina. Additionally, the composite is densified, just after its synthesis, by the application of a mechanical shock. The stresses resulting from these thermal and mechanical shocks must be as more deleterious as the $MoSi_2$ content in the composite is lower. SEM observation has confirmed that the C_3 structure contained more microcracks than the C_2 structure.

The second possible cause is the intergranular phase situated at the alumina matrix grain boundaries. The amount of this phase should be as more important as the alumina content is higher. As this intergranular phase is only partially crystallised, its mechanical properties are lower than that of the main constituents of the composite and it can involve a decrease in elastic moduli of the composites.

Compression creep behaviour

Most of tests performed in the 50-200 MPa stress range have shown a stationary creep stage after some ten hours. The stationary creep rate $\dot{\varepsilon}$ for a stress σ at temperature T is depicted by the Norton-Arrhenius equation :

$$\dot{\varepsilon} = A\,\sigma^n \exp(-E_A/RT) \qquad (7)$$

with n a stress exponent, T temperature, E_A an activation energy, R the ideal gas constant and A a parameter characteristic of the microstructure.

E_A has been evaluated for the three compositions from temperature jump tests under constant stress. Results of jumps at 1200°C and 1400°C under 50 MPa are reported on Figure 6. After each temperature jump, the strain εi, resulting from elastic strain, thermal expansion and creep strain at an inferior temperature has been subtracted from the measured value ε(t).

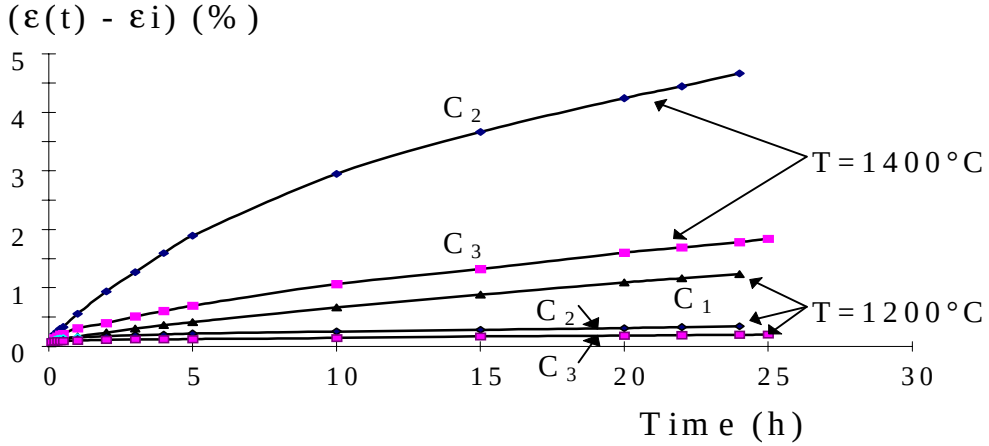

Fig. 6 : Strain versus time under 50 MPa after temperature jumps at 1200°C and 1400°C

For each composite and for the same creep duration, the strain increases for higher temperatures. Whatever the temperature, for the same stress, the strain measured for C_1 is largely superior to the ones measured for C_2 and C_3. There is no result on Figure 6 at 1400°C for C_1 because the jump at this temperature involved a dramatic increase of creep rate with no stationary regime. The variations of $\log\dot{\varepsilon}$ versus 1/T are plotted in Figure 7 for the three composites in order to determine the activation energy from equation (7).

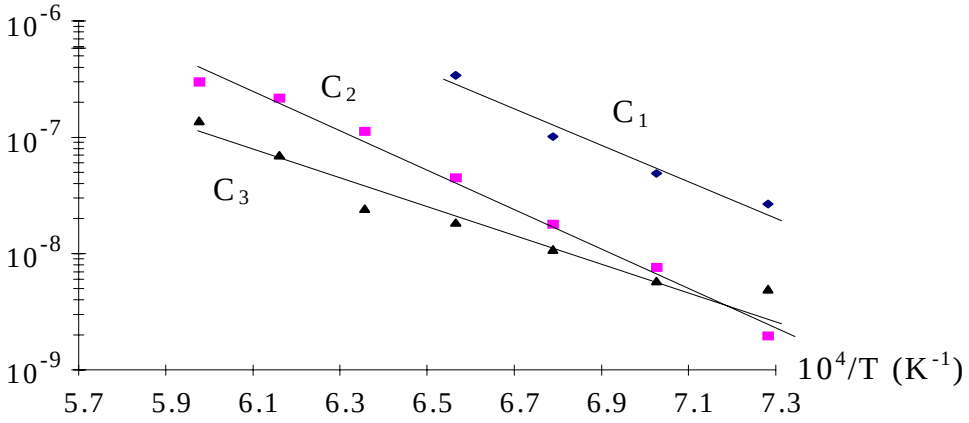

Fig.7: Strain rate versus temperature for the three composites

Table 3 : Values of the activation energy for the three composites and for Al_2O_3 and $MoSi_2$.

Material	$MoSi_2$	C_1	C_2	C_3	Al_2O_3
E_A (kJ/mol)	306 à 430 [11, 12]	289	324	213	416

The results, summed up in table 3, are of same order of magnitude as those found in literature [4, 12-14] for $MoSi_2$ and Al_2O_3-based materials. The lowest value is obtained for C_3, which indicates that C_3 creep rate is less sensitive to temperature than creep rates of composites with lower alumina content.
The determination of the stress exponent n has been made from stress jump tests performed at 1150°C for C_1 and C_2 and at 1200°C for the three composites. Creep rate measurements have been done considering that a constant creep rate was reached after 15 hours. A plot of $\log \dot{\varepsilon}$ versus $\log \sigma$ at 1200°C is given in Figure 8.

Two different regimes seem to be evidenced for the three composites, with a transition at about 100 MPa. The low stress regime is characterised by $n \leq 1$, the high stress regime by $n \approx 4\text{-}5$. A similar behaviour has been observed at 1150°C.

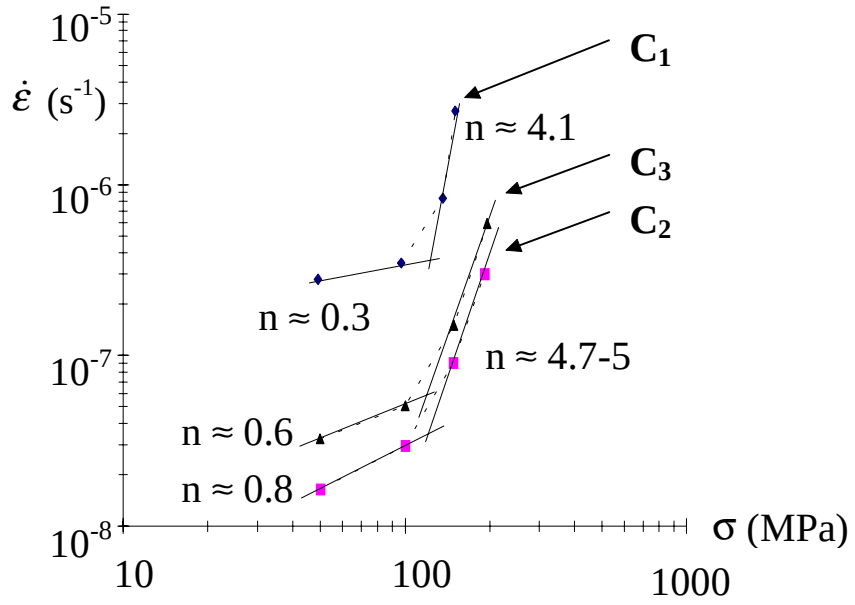

Fig.8 : Results of stress jump tests at 1200°C

However a comparison of results of Figures 7 and 8 shows that creep rates are not the same for a given couple (σ, T) for temperature jump and for stress jump experimentations. The strain rate values obtained during temperature jump tests are, in most cases, inferior to those obtained during stress jump tests. It then appears that, when the composite has remained during a long period (> 24 h) at a temperature superior to 1100°C, the measured creep rate is inferior to the one obtained after 24 hours test for the same temperature-stress conditions. This suggests that a stationary creep stage is not yet achieved because of microstructural evolutions during the tests [5]. As no variation in grain size has been observed, this effect is likely to be linked to an evolution of a vitreous intergranular phase. Nevertheless, it could also be caused by a healing of the cracks under the combined effects of compressive stress and temperature.

A more detailed study (TEM analysis) is needed to identify precisely the creep controlling mechanisms.
Nevertheless, these results are useful to compare the creep resistance of SHS composites with the one of $MoSi_2$ and Al_2O_3. Figure 9 presents the evolutions of creep rate as a function of stress, measured at 1200°C in the same conditions for the three composites and for a dense commercial alumina, as well as results from literature concerning $MoSi_2$ and alumina with an amorphous intergranular phase.

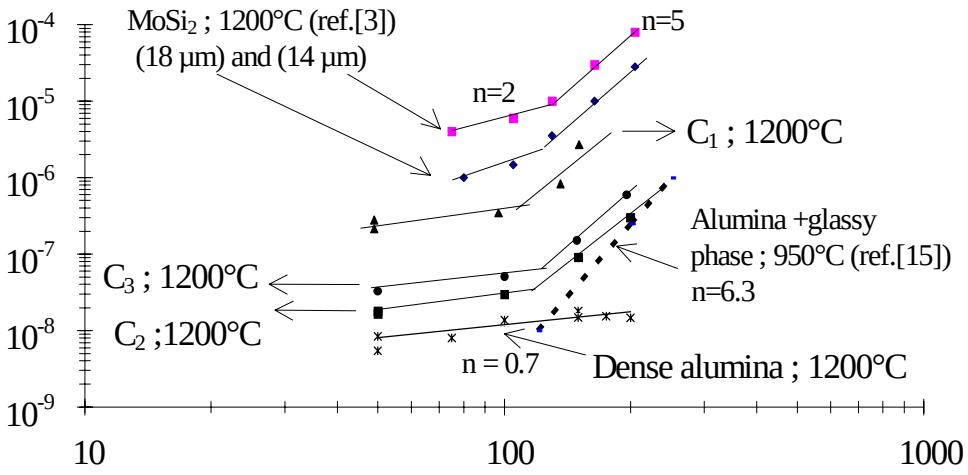

Fig.9: Creep rate versus stress measured for C_1, C_2, C_3 and dense Al_2O_3 at 1200°C; comparison with results from literature for $MoSi_2$ and Al_2O_3

Table 5 sums up stress exponent values calculated from tests at 1200°C (stress jumps tests) and creep rate values obtained under 100 MPa.

Table 5 : Values of calculated stress exponents and of creep rates under 100 MPa at 1200°C

Material	Stress exponent n	Creep rate under 100 MPa
$MoSi_2$ (14 µm) [3]	2 up to 130 MPa ; 5 above	5.10^{-6}
C_1	0.3 up to 100 MPa ; 4.1 above	$3.5.10^{-7}$
C_2	0.8 up to 100 MPa ; 4.7 above	$2.9.10^{-8}$
C_3	0.6 up to 100 MPa ; 5 above	$5.1.10^{-8}$
Dense alumina	0.7	$1.3.10^{-8}$

As expected, strain rate curves of SHS composites are situated between those of dense alumina and $MoSi_2$. Creep curves for the three composites have the same shape as those for $MoSi_2$. C_1 strain rate is one order of magnitude lower than that of $MoSi_2$. Hence, the addition of 21 vol. % Al_2O_3 considerably reinforces $MoSi_2$ creep resistance at 1200°C.
The stress exponent values seem to indicate that :
- for the three composites under low stresses (<100 MPa), as for dense alumina, the stress exponent is close to 1, which corresponds to a creep strain controlled by grain boundary sliding accomodated by diffusion phenomena [7];
- under high stresses (> 100 MPa), stress exponent values between 4 and 5 are characteristic of a creep strain controlled either by dislocation or by cavitation mechanisms [16]. In the case of C_1, $MoSi_2$ can contribute to creep strain in facilitating dislocation glide and climb. In the

case of C_2 and C_3, the amorphous intergranular phase may contribute to cavitation mechanisms. TEM observations would be necessary to conclude concerning the creep mechanisms of SHS composites. Nevertheless, SEM observations of C_3 samples after creep tests show the presence of large pores, which would indicate that cavitation mechanisms could be responsible for the creep strain of composite C_3.

CONCLUSION

$MoSi_2$-Al_2O_3 composites processed by SHS exhibit interesting mechanical properties, intermediate between those of pure $MoSi_2$ and pure Al_2O_3. Further work is still needed to improve the microstructure, in particular to control the amount of intergranular phases and/or the density of microcracks after processing, which are responsible for a decrease of elastic moduli and for an evolution of creep rate during the pseudo-stationary creep stage. Nevertheless, these materials have been found to present attractive thermal and electrical properties [5]. In particular the electrical conductivity of the C_1 composition remains of the same order of magnitude than the one of pure $MoSi_2$, with a much better creep behaviour. Therefore, these materials are candidates for making heating components with improved reliability.

AKNOWLEDGEMENT

The authors are grateful to Professor J-L Besson from SPCTS Laboratory (Limoges, France) for helpful discussions about creep experimentations.

REFERENCES

1. Pope, D.P. and Darolia, R., "High-temperature applications of intermetallic compounds", *MRS Bulletin*, 5, 1996, pp. 30-36.

2. Chou, T.C. and Nieh, T.G., "Mechanism of $MoSi_2$ pest during low temperature oxidation", *J. of Mater. Res.*, 8, 1, 1993, pp. 214-226.

3. Petrovic, J.J., "High temperature structural silicides", *Ceram. Eng. and Sci. Proc.,* 18, 3, 1997, pp. 3-17.

4. Vasudevan, A.K. and Petrovic, J.J., "A comparative overview of molybdenum disilicide composites", *Mater. Sci. and Eng.*, A155, 1992, pp. 1-17.

5. Dumont, A.L., "Composites $MoSi_2/Al_2O_3$: élaboration à partir de réactions auto-entretenues (SHS) et caractérisations", *Thesis,* Limoges University, France, 1999.

6. Dumont, A.L., Smith, D.S., Gault, C., Bonnet, J.P., "Preparation and densification of $MoSi_2/Al_2O_3$-based composites using self-propagating high-temperature synthesis", *Intern. J. of Self-Propagating High-Temp. Synthesis,* 7, 2, 1998, pp. 269-279.

7. Jeng, Y.L., Lavernia, E.J., Review "Processing of molybdenum disilicide", *J. Mater. Sci.,* 29, 1994, p 2557-2571.

8. Nakamura, M., Matsumoto, S., Hirano, T., "Elastic Constants of $MoSi_2$ and WSi_2 single crystals", *J. Mater. Sci.*, 25, 1990, p 3309-3313.

9. Spriggs, R.M., "Expression for Effect of Porosity on Elastic Modulus of Polycristalline Refractory Materials, Particularly Aluminum Oxide", *J. Am. Ceram. Soc.- Discussions and Notes*, Dec. 1961, p 628-629.

10. Peselnick, L., Meister, R., "Variational Method of Determining Effective Moduli of Polycrystals : (A) Hexagonal Symmetry, (B) Trigonal Symmetry", *J. Appl. Phys.*, 36, 9, 1963, p 2879-2884.

11. Neergaard, L.J., Petrovic, J.J., "Fracture behaviour of $MoSi_2/Si_3N_4$ composite", *Ceram. Eng. and Sci. Proc.*, 16, 4, 1995, p 137-146.

12. Sadananda, K., Feng, C.R., Jones, H.N., Petrovic, J.J., "Creep of molybdenum disilicide composites", *Mater. Sci. and Eng.*, A155, 1992, p 227-239.

13. Yoshida, H., Ikuhara, Y., Sakuma, T., "High-temperature creep resistance in rare-earth-doped fine-grained Al_2O_3", *J. Mater. Res.*, 13, 9, 1998, p 2597-2601.

14. Cannon, R.M., Rhodes, W.H., Heuer, A.M., "Plastic deformation of fine grained alumina (Al_2O_3) : I, Interface-controlled diffusional creep", *J. Am. Ceram. Soc.*, 63, 1-2, 1980, p 46-53.

15. Clarke, D.R. "High-temperature deformation of a polycristalline alumina containing an intergranular glass phase", *J. Mater. Sci.*, 20, 1985, p 1321-1332.

16. French, J.D. , Wiederhorn, S.M. , Petrovic, J.J.,"Tensile Creep and Creep rupture of SiC-Reinforced $MoSi_2$", *Ceram. Eng. and Sci. Proc.*, 16, 4, 1995, p 129-136.